DOI: 10.1002/ejic.201100116

Synthesis and Characterization of a Series of Ruthenium Tris(β-diketonato) Complexes by an UHV-STM Investigation and Numerical Calculations

Sabrina Munery,[a] Nicolas Ratel-Ramond,[a] Youness Benjalal,[a] Loranne Vernisse,[a] Olivier Guillermet,[a] Xavier Bouju,[a] Roland Coratger,[a] and Jacques Bonvoisin*[a]

Keywords: Ruthenium / β-Diketonato complexes / Adsorption

A series of ruthenium tris(β-diketonate) complexes was investigated by using electrochemistry, UV/Vis spectroscopy, ^{1}H NMR and ^{13}C NMR spectroscopy and FAB mass spectroscopy. Several new mononuclear mixed-ligand ruthenium(III) complexes were prepared: with three dibenzoylmethanate ions (dbm) {[Ru(dbm)$_3$] (**1**)}, one or two acetylacetonate ions (2,4-pentanedionate, acac) {[Ru(dbm)$_2$(acac)] (**2**), [Ru(dbm)(acac)$_2$] (**3**)}, two acetonitrile ligands {[Ru(dbm)$_2$-(CH$_3$CN)$_2$][CF$_3$SO$_3$] (**4**)} or a functionalized acetylacetonate ion {[Ru(dbm)$_2$(acac-I)] (**5**) (acac-I = 3-iodo-2,4-pentanedionate ion), [Ru(dbm)$_2$(acac-Br)] (**6**) (acac-Br = 3-bromo-2,4-pentanedionate ion)}. In addition, X-ray structures for complexes **1**, **2**, **3**, **4** and **6** were determined. Scanning tunnelling microscopy measurements at liquid He temperature and in an ultra-high vacuum (UHV-STM) were conducted on complex **1** on a Ag(111) surface. This indicates that the complex can be successfully evaporated and observed after adsorption onto a metallic substrate. Analysis of the STM images, supported by adsorption and STM image calculations, demonstrates that the molecules exist in two stable forms when adsorbed onto the surface.

Introduction

Coordinated metal ions are the essential centres of chemical activity in a variety of molecules. Beyond any chemical application, metal complexes embedded into supramolecular assemblies are potential building blocks for molecular electronics.[1–8] Therefore, studying the functional molecules on a substrate and investigating their behaviour and properties are primary requirements for potential applications, since the molecular deformation due to surface interaction plays a crucial role.[9–11] New progress and possibilities in using metal complexes for molecular electronics has been reviewed recently, highlighting that the electronic state of metal complexes is attractive for conducting highly integrated, functional molecular components.[12] In recent years, the investigation of the properties of isolated, individual molecules has been greatly facilitated by scanning tunnelling microscopy (STM). Thus, this technique has been used to study the adsorption site and geometry of molecules on the surfaces,[9,13] to obtain high resolution images of the intramolecular structure,[14–16] to investigate the electronic properties of individual molecules,[17–19] to detect different spin states of transition-metal complexes[20] and to observe charge localization on isolated mixed-valence complexes.[21–23] A recent review also appeared on STM spectroscopy of magnetic molecules.[24] Several studies have been reported on ruthenium compounds measured by STM[25–36] and also on ruthenium and tris(diketonato) ligands,[37–42] but very few on adsorption of ruthenium or metal acetylacetonate (acac) complexes and their derivatives.[43,44] It is then of interest to synthesize and characterise Ru complexes including ligands that are favoured for their evaporation and adsorption for further investigations using STM and related techniques such as scanning tunnelling spectroscopy. This is the reason for choosing the dibenzoylmethanato (dbm) ligand, mainly because of its propensity to adhere to the substrate as a result of its phenyl rings.[45,46]

In this work, we report on the synthesis and characterization of a series of mononuclear ruthenium complexes with dbm ligands and functionalized or non-functionalized acac ligands. We also present a study of the adsorption of a ruthenium tris(β-diketonate) complex at low temperature, i.e. tris(dibenzoylmethanato)ruthenium [Ru(dbm)$_3$] (**1**) on a Ag(111) surface by UHV-STM coupled to molecular adsorption calculations and STM image calculations. These calculations have been done to obtain unambiguous information of the adsorption state. Indeed, it is necessary to compare experimental images to theoretical STM ones preceded by molecular mechanics calculations.[11]

Results and Discussion

A series of Ru^{III} tris(β-diketonato) complexes have previously been synthesized.[37,47,48] Complex **1** has already

[a] CNRS, CEMES and MANA Satellite, GNS,
29 rue Jeanne Marvig, B. P. 94347, 31055 Toulouse Cedex 4, France
Fax: +33-5-62257999
E-mail: jbonvoisin@cemes.fr

Supporting information for this article is available on the WWW under http://dx.doi.org/10.1002/ejic.201100116.

been obtained in 47% yield by Endo et al.,[47] starting from a "Ruthenium blue solution". Here, we present a synthesis where the three compounds **1**–**3** can be obtained in a one-pot reaction (see Scheme 1) starting from ruthenium trichloride, 2 equiv. of dbm and 1 equiv. of acac. Each compound was separated and purified by column chromatography. Complex **2** can also be obtained from another method (see Scheme 2), but with lower yield, by the preparation of the bis(MeCN)bis(β-diketonato)ruthenium(III) species through a ligand displacement reaction of tris(β-diketonato)ruthenium(III) complexes, induced by strong acid.[49,50] The iodination or bromination selectively occurred at the γ-position of the acac ligand and led to compounds **5** and **6** in good yield (77 and 89%, respectively); this was adapted from literature procedures.[51–53]

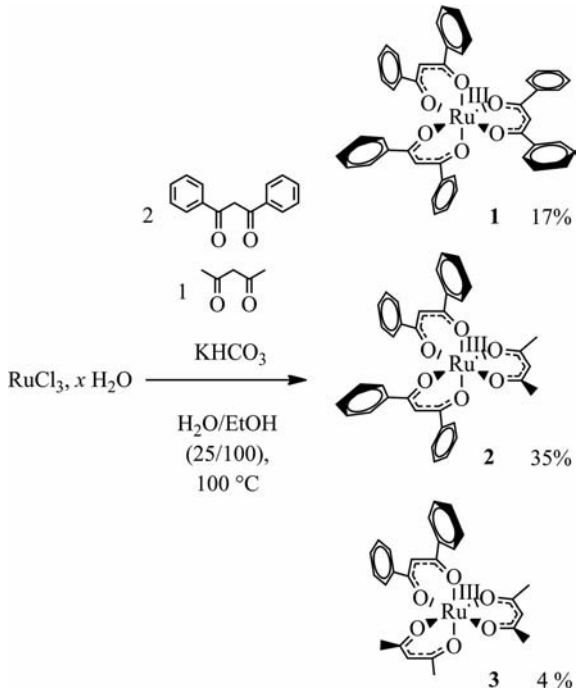

Scheme 1. Synthesis of complexes **1**–**3**.

Cyclic voltammetry (CV) data for complexes **1**–**6** are given in Table 1 and also in Figure S1. The $E_{1/2}$ potentials were determined from the average of the anodic and cathodic peak potentials. All the waves are reversible with peak to peak separation of around 60–80 mV. The reversible half-wave potentials $E_{1/2}$ of **5**–**6** are 50–63 mV (76–81 mV) more positive than that of **2** for the Ru^{IV}/Ru^{III} (Ru^{III}/Ru^{II}) redox couple. These positive shifts of the potentials reflect the electron-withdrawing character of –I and –Br.

The UV/Vis data are shown in Table 1. Complexes **1**–**3**, **5** and **6** present the same overall shape but differ in intensity (see Figures S5 and S6, Supporting Information). They all present three strong bands in the UV/Vis area. One can notice that when going from **1** to **3**, the transition intensity around 330 nm decreases successively by a factor of one third. This corresponds to the progressive replacement of dbm by the acac ligand.

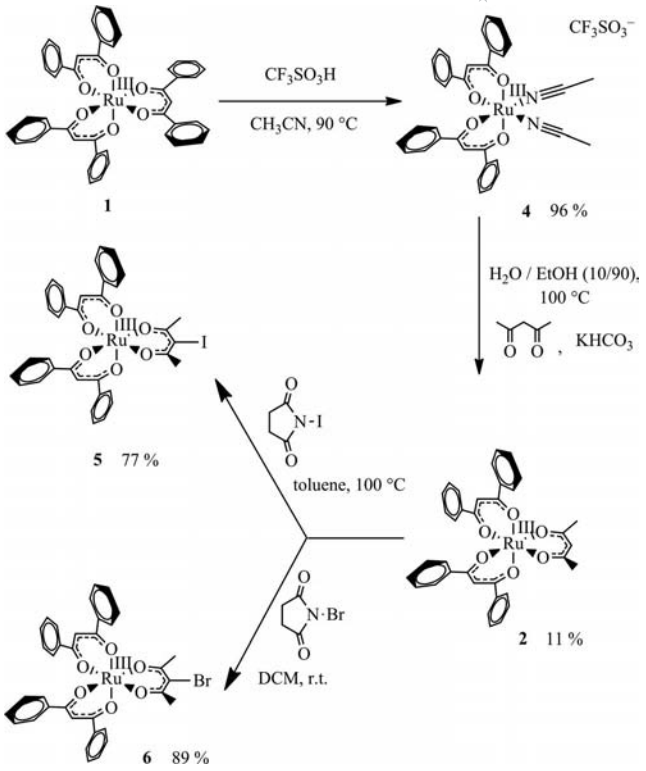

Scheme 2. Synthesis of complexes **2**–**5** and **6**.

Table 1. UV/Vis and electrochemical data.

Complex	UV/Vis data[a] λ [nm] (ε [$M^{-1}cm^{-1}$])	Redox potentials[b] $E_{1/2}$ [V] (ΔE [V]) Ru^{III}/Ru^{II}	Ru^{IV}/Ru^{III}
1	430 (12847) 330 (48907) 258 (35503)	–0.615 (0.068)	1.000 (0.076)
2	415 (8761) 332 (34805) 258 (28077)	–0.689 (0.073)	0.995 (0.076)
3	504 (2240) 404 (6524) 335 (20646) 262 (20635) 229 (13510)	–0.767 (0.078)	0.993 (0.081)
4	633 (1781) 388 (11862) 336 (37570) 263 (20931) 228 (16234)	0.150 (0.063)	
5	562 (2256) 414 (10569) 331 (36727) 257 (27886) 228 (23069)	–0.613 (0.073)	1.045 (0.074)
6	556 (2417) 412 (11644) 331 (40967) 258 (30580) 228 (22823)	–0.608 (0.074)	1.058 (0.073)

[a] In CH_2Cl_2. [b] vs. SCE, in CH_2Cl_2, 0.1 M TBAH, 0.1 Vs^{-1}.

NMR experiments have been performed on complexes **1**–**3**, **5** and **6**. All the NMR (^{1}H and ^{13}C) spectra are shown in the Supporting Information (see Supporting Information, Figures S7–S16). All the ^{1}H and ^{13}C NMR signals were unambiguously assigned on the basis of chemical shifts, spin-spin coupling constants, splitting patterns and signal intensities by using ^{1}H-^{1}H COSY; they are presented in the Exp. Section for complexes **1**–**3**, **5** and **6**. A comparison of the ^{1}H NMR spectra for complexes **1**, **2** and **6** is shown in Figure 1. Ru^{III} complexes often give very broad, poorly resolved ^{1}H NMR signals as a result of rapid nuclear spin relaxation induced by the paramagnetism, but examples of interpretable ^{1}H NMR spectroscopic data for Ru^{III} species have appeared.[37,47] The spectrum of $[Ru(dbm)_3]$, which has a D_3 symmetry, is simple: it consists of four peaks, three from the phenyl protons and one from the methyne protons of the ligands in accordance with the work of Endo et al.[47] The signal of the methyne protons for all the ruthenium(III) complexes appears at a very high-field region because of the paramagnetism of the ruthenium(III) complexes. On going from complex **1** to complex **2** all the phenyls protons are doubled because of the loss of symmetry. The δ values for the Me signals of the coordinated acac ligands reveal an upfield shift (compared to a "diamagnetic value") because of the interaction with the paramagnetic Ru^{III} centre. It has to be noted that the methyne signal (δ = –22.8 ppm) of the coordinated acac ligand is less upfield than that of the methyne signals (δ = –37.0 ppm) of the dbm ligands. As expected, the methyne signal of the coordinated acac ligand for complex **6** no longer occurs.

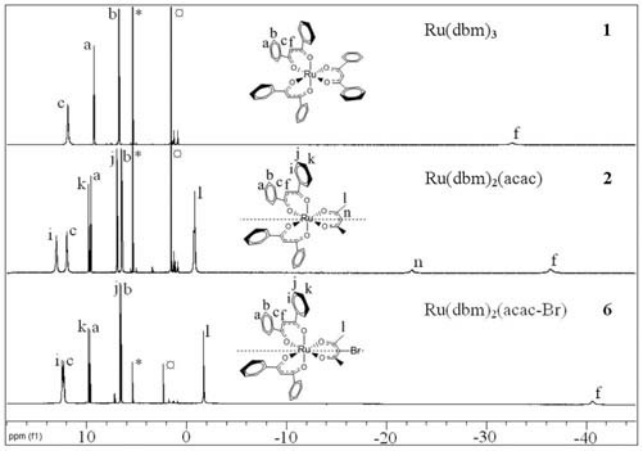

Figure 1. ^{1}H NMR spectra of complexes **1**, **2** and **6** in CD_2Cl_2 at room temp. (* and ¤ refer to the deuterated solvent and traces of impurities in the solvent, respectively).

Crystal structure data for complexes **1**–**4** and **6** are given in Table S1 (see Supporting Information). Selected bond lengths and angles are reported in Tables S2 and S3. Figures 2 and 3 show the ORTEP drawings of **1** and **6**, respectively. The Ru–O distances as well as the bond angles are consistent with the range of values reported in the literature.[37,54,55]

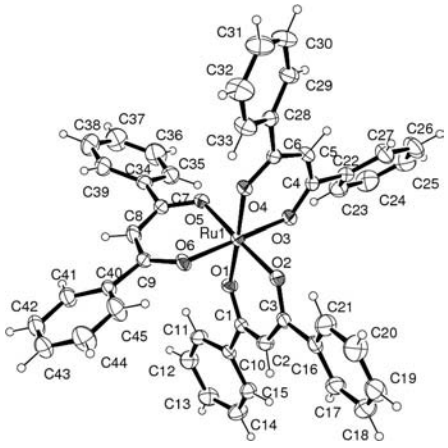

Figure 2. ORTEP drawing of $[Ru(dbm)_3]$ (**1**) (30% probability of thermal ellipsoids).

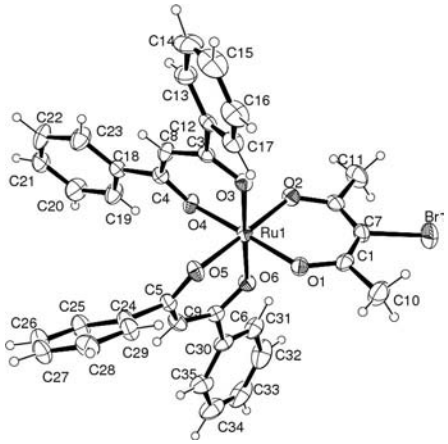

Figure 3. ORTEP drawing of the $[Ru(dbm)_2(acac\text{-}Br)]$ (**6**) (30% probability of thermal ellipsoids).

STM Experiments

After evaporation of $[Ru(dbm)_3]$ (**1**) on Ag(111) kept at 4.5 K, the surface is covered with two different objects always presenting the same shape. This shows that the molecules are not destroyed during evaporation since no fragments appear on the substrate while scanning with the STM tip. It should be noted that the general shape of these two forms does not dramatically change in terms of bias voltage in the –2 to +2 V range. As we will see further, calculations confirm that molecules stay intact on the surface. Three of these objects (labelled 1, 2 and 3) are shown in Figure 4 (a).

In type (1), the molecule exhibits a two-lobed structure with an apparent height of about 3.9 Å (see part b of Figure 4, red curve). The two protrusions are separated by about 0.87 nm while the overall size of the molecule is 1.92 nm. Two small corrugations also appear on the sides of the main protrusions giving an apparent square shape to the structure in "contact" with the surface. The other two objects present a different structure. A central three-lobed structure is surrounded by three smaller bumps, each of them making an angle of 25° with respect to the threefold axes of symmetry imposed by the central core. The objects

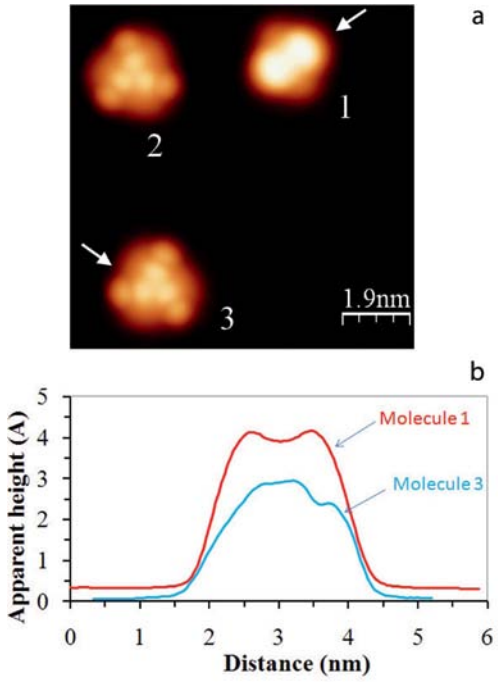

Figure 4. a: STM image (9.4 × 9.4 nm^2) of the Ag(111) surface after evaporation of Ru(dbm)$_3$ on a substrate held at liquid helium temperature (sample bias voltage 1.5 V, tunnelling current 15 pA, T = 4.5 K). The two arrows indicate the directions in which the cross sections in part b have been performed. b: Cross sections along molecule 1 and molecule 3 showing an apparent height above the Ag(111) surface of about 3.9 and 2.9 Å, respectively. The red curve has been vertically shifted for clarity.

(2) and (3) differ by the fact that the rotation of the peripheral groups is anticlockwise in (2) and clockwise in (3), which reveals the chiral character of these adsorbates on the surface.

The cross section presented in Figure 4 (b, blue curve) shows that the apparent height is about 2.89 Å (for these tunnelling conditions) while the lateral size is 2 nm. The corrugation of the peripheral groups is 0.55 Å below the central part of the molecule. A racemic mixture of species (2) and (3) has been observed on the substrate indicating that the adsorption process is not enantioselective for this molecule on the (111) substrate. One has to note that these racemic forms represent about 20% of the total imaged molecules.

Adsorption and STM Image Calculations

The adsorption for the Ru(dbm)$_3$ molecule was carried out with an extended semi-empirical atom superposition and electron delocalization (ASED+) approach.[56] Standard parameters for carbon, hydrogen and oxygen were used. The (H_{ii}, ζ) extended Hückel parameters for Ru were chosen as Ru 5s (–8.6, 2.078), Ru 5p (–3.28, 2.043) and Ru 4d H_{ii} = –11.12 eV, ζ_1 = 5.378 and ζ_2 = 2.303 with weighting coefficients of 0.534 and 0.6365, respectively, taken from Hoffmann et al.[57] After relaxation of the geometry of the molecule on the surface, two different structures were found. It is notable that the optimization procedure was carried out with a number of starting positions in order to accurately investigate the adsorption potential energy surface.

In the first structure (Figure 5), the two dbm groups were placed parallel to the plane of the Ag(111) surface. After relaxation with ASED+, the molecular structure exhibits two phenyl rings perpendicular to the surface plane (Figure 5, b). The adsorption energy was found to be 0.60 eV where all the atoms closest to the surface are at a height of 2.5 Å. In the second structure (Figure 6), the molecule was placed on the surface with three phenyl groups exhibiting an octahedral geometry and with each oxygen atom above a hollow site on the Ag(111) surface. The relaxed structure is shown in Figure 6 (b) where all the atoms closest to the surface are at a height of 2.5 Å. The adsorption energy including the van der Waals interaction between the molecule and the metallic surface reaches 0.34 eV.

Adsorption calculations give two stable conformations, the two-lobed structure being favoured. This is in good agreement with the statistical experimental results. It is worth to be highlighted that the central cage around the Ru atom is not distorted in the two forms. Indeed, among all the starting configurations we tried, it appears that the stability of the central octahedral site is a key point for the final conformation. Moreover, we were not able to characterise the energy barrier between the two final adsorption states because of the large number of degrees of freedom of the molecule.

The STM images of a Ru(dbm)$_3$ molecule were calculated with the elastic quantum chemistry scattering technique (ESQC)[58] under the same tunnelling conditions as in the STM experiments. The calculated results displayed in

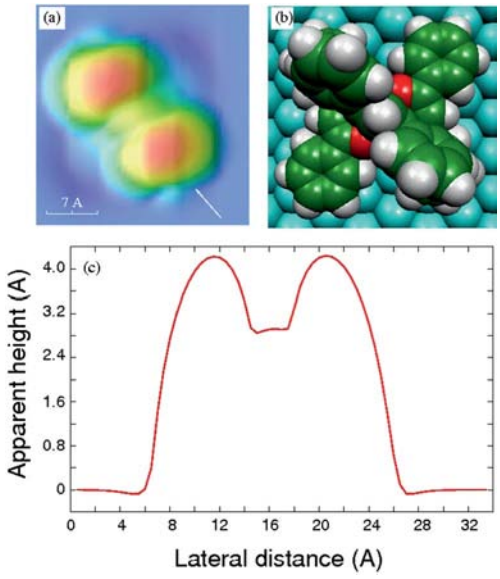

Figure 5. a: EHMO-ESQC calculated image of Ru(dbm)$_3$ molecule adsorbed on Ag(111) under the same tunnelling conditions as in the experimental STM. b: Space-filling model of Ru(dbm)$_3$ adsorbed on Ag(111). c: Profile showing the calculated apparent height (4.22 Å) of the molecule shows that the two bright protrusions are separated by about 9 Å.

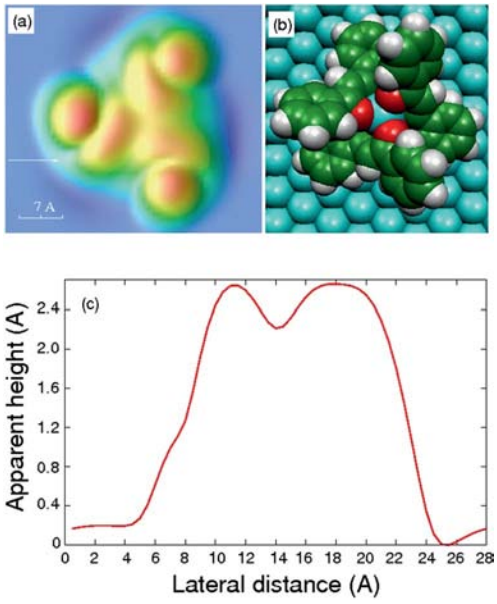

Figure 6. a: EHMO-ESQC calculated image of $Ru(dbm)_3$ adsorbed on Ag(111) under the same tunnelling conditions as in the experimental STM. b: Space-filling model of $Ru(dbm)_3$ adsorbed on Ag(111). c: Profile showing the calculated apparent height of the $Ru(dbm)_3$ molecule with respect to the Ag(111) surface (2.66 Å) as indicated by an arrow in part a.

Figures 5 and 6 are consistent with the experimental results. This corroborates the fact that the molecules are not destroyed during the deposition process.

As already found for "Lander" molecules, the contrast in the STM images is governed by the topmost phenyl rings modulated by the presence of the oxygen atoms underneath.[13,59]

This suggests that the two forms observed in the STM images result from two different adsorption geometries due to the peculiar 3D structure of complex **1**.

Conclusions

Ruthenium complexes have been characterised using electrochemistry, UV/Vis spectroscopy, ^{1}H NMR and ^{13}C NMR spectroscopy and FAB mass spectroscopy. The main objective was to synthesize compounds with magnetic and electron transport properties and single [$Ru(dbm)_3$] molecules have been observed by low-temperature STM. The STM images as well as the calculations indicate that the molecules exhibit two different adsorption geometries on the Ag(111) surface and that their stability can be attributed to the dbm ligand interacting with the substrate. More generally, these results show that this type of compound can be used for experiments in which single larger Ru complexes would be studied and manipulated using the special properties of STM for potential applications in the field of quantum computation. Moreover, it opens the route to the physics of the Kondo effect on the single molecular scale,[60–62] in particular because of the presence of the Ru^{III} paramagnetic centre, or to studies dedicated to the magnetic information transfer through a molecular adlayer or molecular wire.[63–65]

Experimental Section

Materials: All chemicals and solvents were of reagent grade or better. The complexes were purified by column chromatography using silica gel 60 (Merck or Agela). Elemental analyses were performed by the Service de microanalyse ICSN-CNRS Gif/Yvette.

Physical Measurements: UV/Vis spectra were recorded with a Varian Cary 5000 spectrophotometer. Cyclic voltammograms were obtained with an Autolab system (PGSTAT100) in CH_2Cl_2 (0.1 M tetrabutylammonium hexafluorophosphate, TBAH as supporting electrolyte) at 25 °C. A three-electrode cell was used comprising a 1 mm Pt-disk working electrode, a Pt-wire auxiliary electrode and an aqueous saturated calomel (SCE) reference electrode. Mass spectra were recorded by the "Service de Spectroscopie de Masse" of Paul Sabatier University using FAB mass spectroscopy (Nermag R10-R10, NBA matrix) in the positive mode. ^{1}H NMR spectra were performed with Bruker Avance 300 MHz and 500 MHz spectrometers in CD_2Cl_2.

STM Studies: STM experiments have been performed at $T = 4.5$ K on an ultra-high vacuum STM (LT-Omicron) with a base pressure of 1.5×10^{-11} mbar. The Ag(111) crystal is cleaned by repeated Ar^+ bombardment cycles followed by annealing at 810 K. The molecules are evaporated from a 0.15 mm tungsten filament submitted to high temperature outgassing cycles before the evaporations. The latter was conducted while the substrate was held at liquid helium temperature, i.e. directly on the STM head. In this case, the vacuum never exceeds 1.4×10^{-10} mbar in the STM chamber. Tips made of 200-μm diameter tungsten wires were prepared by electrochemical etching in a 1 M NaOH solution and were cleaned in the UHV preparation chamber using direct current heating. All the STM images presented in this paper are given without any data processing.

X-ray Diffraction Studies: All the crystals were obtained either by slow evaporation of a solution of CH_2Cl_2/pentane (for **1**, **2** and **4**) or precipitation at low temperature (for **3** and **6**). Suitable crystals were first selected under a microscope and then mounted onto a goniometer head using cyanolite. The diffraction data were collected using an Enraf Kappa-CCD automatic X-ray single crystal diffractometer, using Mo-K_α radiation, for which a graphite monochromator was used. Intensities were measured using an Apex2 detector at a sample to detector distance of 40 mm. The crystallographic cell was found using EVAL-CCD.[66] The point group determination was followed by the determination of the position of all non-hydrogen atoms by direct methods using SIR2004[67] and refined in the WinGX software package[68] using SHELX-97.[69] Absorption corrections were performed using the SADABS program.[70,71] The refined cell constants and additional crystal data are given in Table S1. The non hydrogen atoms were easily localized after structure determination and subsequent Fourier analyses revealed the position of the hydrogen atoms. The latter were introduced as riding with their relevant parent atoms. The refinements were performed using anisotropic thermal displacement parameters for all the non-hydrogen atoms.

CCDC-803933 (for **1**), -803944 (for **2**), -803947 (for **3**), -803948 (for **4**), and -803955 (for **6**) contain the supplementary crystallographic data for this paper. These data can be obtained free of charge from The Cambridge Crystallographic Data Centre via www.ccdc.cam.ac.uk/data_request/cif.

Synthesis of the Complexes

[Ru(dbm)$_3$] (1): [Ru(dbm)$_3$] (**1**) was prepared from a slightly modified procedure taken from Endo et al.:[48] $RuCl_3 \cdot xH_2O$ (1 g, 4.1 mmol as Ru) was solubilised in the solvent mixture ethanol/water (100:25; 125 mL) previously degassed with argon. The reaction mixture was stirred at 100 °C and became dark blue in colour over 4–5 h. Dbm (3.3 g, 14.7 mmol) was added to the cooled solution. A portion of $KHCO_3$ (0.78 g, 7.8 mmol) was added to the cooled solution 1.5 h after the addition of the ligand to the ruthenium blue solution, which had become green. The colour of the solution turned gradually from green to orange leaving a dark precipitate. Another portion of $KHCO_3$ (0.75 g, 7.5 mmol) was added 1 h after the first addition, at which point the solution was already orange. Each time $KHCO_3$ was added gas formation was observed. The solution was refluxed for an additional 2 h. At the end of the reaction the dark precipitate was filtered and washed with cold ethanol and pentane until the ligand spot was no longer visible on the TLC plate. The complex was purified using column chromatography on silica with a mixture of cyclohexane/CH_2Cl_2 (70:30). A black solid was obtained after evaporation with a yield of 47% (1.6 g). Mass spectroscopy (FAB, DCM, MNBA) *m*/*z* = 771 M^+ (calcd. 770.81), 548 [M – dbm]$^+$. IR (KBr): $\tilde{\nu}$ = 1520 (C=O), 1598, 1586 and 1483 (C=C) cm^{-1}. CV (DCM, 0.1 M TBAH, 0.1 V s^{-1}, vs SCE) $E_{1/2}(Ru^{III}/Ru^{II})$ = –0.615 V, $|\Delta E|$ = 0.068 V, $E_{1/2}(Ru^{III}/Ru^{IV})$ = 1.000 V, $|\Delta E|$ = 0.076 V. UV/Vis spectroscopy (DCM, 4.67×10^{-5} M): λ (ε/10^3 M^{-1} cm^{-1}) = 430 (12.8), 330 (48.9), 258 (35.5) nm. ^{1}H NMR (CD_2Cl_2): δ = 5.32, 11.94 (s, 12 H, H_c), 9.28 (t, *J* = 7.0 Hz, 6 H, H_a), 6.76 (d, *J* = 7.0 Hz, 12 H, H_b), –33.12 (s, 3 H, H_f) ppm. ^{13}C NMR (CD_2Cl_2): δ = 53.7, 135.64 (b), 125.50 (a), 113.79 (c), 100.63 (d) ppm.

[Ru(dbm)$_2$(CH$_3$CN)$_2$]CF$_3$SO$_3$ (4): [Ru(dbm)$_2$(CH$_3$CN)$_2$]CF$_3$SO$_3$ (**4**) was synthesized according to the procedure given by I. R Baird et al.[50] A particularly notable colour change from red-brown to green was observed. Yield = 96%, 1 g) Mass spectroscopy (FAB, DCM, MNBA) *m*/*z* = 630 [M – CF_3SO_3]$^+$ (calcd. 629.67), 589 [M – CH_3CN]$^+$, 548 [M – 2 CH_3CN]$^+$. IR (KBr): $\tilde{\nu}$ = 1523 (C=O), 1598, 1587 and 1484 (C=C), 2325 and 2297 (C≡N), 2992 and 2927 (CH sp^3) cm^{-1}. CV (DCM, 0.1 M TBAH, 0.1 V s^{-1}, vs SCE) $E_{1/2}(Ru^{III}/Ru^{II})$ = 0.150 V, $|\Delta E|$ = 0.063 V, E_{ox} = 1.724 V. UV/Vis spectroscopy (DCM, 4.94×10^{-5} M): λ (ε/10^3 M^{-1} cm^{-1}) 633 (1.8), 388 (11.9), 336 (37.6), 263 (20.9), 228 (16.2) nm.

[Ru(dbm)$_2$(acac)] (2) and [Ru(dbm)(acac)$_2$] (3): [Ru(dbm)$_2$(acac)] (**2**) was prepared by two different procedures (see Schemes 1 and 2).

First, the complex was prepared from [Ru(dbm)$_2$(CH$_3$CN)$_2$]CF$_3$SO$_3$ (**4**) (0.8 g, 1.03 mmol) solubilised in a solvent mixture of ethanol/water (90:10, 100 mL) previously degassed with argon. acac (0.135 mL, 1.3 mmol) and $KHCO_3$ (0.13 g, 1.3 mmol) were added. The reaction mixture was stirred at 100 °C. The colour of the solution turned from green to pink-red in about 15 min after reflux. After 1 h the TLC plates no longer showed the spot for [Ru(dbm)$_2$(CH$_3$CN)$_2$]CF$_3$SO$_3$, and thus the reaction was stopped. The solution was evaporated to dryness. To remove the solution's salts, the crude product was extracted with ca. 40 mL portions of dichloromethane and ca. 3 × 20 mL portions of water. The extract was evaporated to dryness. Then it was purified by column chromatography on silica, first with toluene, followed by a mixture of hexane/CH_2Cl_2 (70:30) to give black crystals (yield 11%, 80 mg).

In the second procedure, inspired by that given by Endo et al.,[48] $RuCl_3 \cdot xH_2O$ (2 g, 8.2 mmol) was solubilised in the solvent mixture ethanol/water (125:30, 155 mL) previously degassed with argon. The reaction mixture was stirred at 100 °C and turned dark blue in colour over 4–5 h. At this time, dbm (3.7 g, 16.5 mmol) and acac (0.844 mL, 8.2 mmol) were added to the cooled solution. TLC was used to check the reaction on silica with toluene. The solution was refluxed for an additional 2 h. Then, the mixture was cooled again and $KHCO_3$ (1.25 g, 12.5 mmol) was added to the green solution. A release of gas was observed. During the night, the solution turned to orange and in the morning, it was cooled to add another portion of $KHCO_3$ (1.23 g, 12.3 mmol). The solution was put under reflux yet again for 4 h, and then the last portion of $KHCO_3$ (1.24 g, 12.4 mmol) was added to the cooled solution. A black precipitate gradually appeared with the addition of $KHCO_3$. The heating and the stirring were kept constant for a second night. The reaction was stopped after 48 h. The solvents were evaporated and the black precipitate was purified using column chromatography on silica with a mixture of hexane/CH_2Cl_2 (60:40). Three products were collected: first, [Ru(dbm)$_3$] (**1**) (black powder, yield 17%, 1.1 g), second, [Ru(dbm)$_2$(acac)] (**2**) (crimson powder, yield 35%, 1.9 g) and third, [Ru(dbm)(acac)$_2$] (**3**) (dark-red crystals, yield 4%, 0.16 g). [Ru(dbm)$_2$(acac)] (**2**), $C_{35}H_{29}O_6Ru$ (646.67): calcd. C 65.0, H 4.5, Ru 15.6; found C 64.0, H 4.7, Ru 13.0. Mass spectroscopy (FAB, DCM, MNBA) *m*/*z* = 647 M^+ (calcd. 646.67), 548 [M – acac]$^+$, 424 [M – Dbm]$^+$. IR (KBr): $\tilde{\nu}$ = 1520 (C=O), 1598 and 1483 (C=C), 2960 and 2921 (CH sp^3) cm^{-1}. CV (DCM, 0.1 M TBAH, 0.1 V s^{-1}, vs SCE) $E_{1/2}(Ru^{III}/Ru^{II})$ = –0.689 V, $|\Delta E|$ = 0.073 V, $E_{1/2}(Ru^{III}/Ru^{IV})$ = 0.995 V, $|\Delta E|$ = 0.076 V. UV/Vis spectroscopy (DCM, 5.41×10^{-5} M): λ (ε/10^3 M^{-1} cm^{-1}) = 415 (8.8), 332 (34.8), 258 (28.1) nm. ^{1}H NMR (CD_2Cl_2): δ = 5.32, 13.10 (s, 4 H, H_i), 12.04 (s, 4 H, H_c), 9.81 (t, *J* = 6.9 Hz, 2 H, H_k), 9.60 (t, *J* = 6.9 Hz, 2 H, H_a), 6.95 (d, *J* = 6.8 Hz, 4 H, H_j), 6.42 (d, *J* = 6.8 Hz, 4 H, H_b), –0.80 (s, 6 H, H_l), –22.75 (s, 1 H, H_n), –37.02 (s, 2 H, H_f) ppm. ^{13}C NMR (CD_2Cl_2): δ = 53.7, 137.62 (b), 137.20 (j), 124.09 (k), 122.65 (a), 111.99 (i), 109.19 (d), 108.91 (c), 103.76 (h), –32.69 (l) ppm. [Ru(dbm)(acac)$_2$] (**3**), $C_{25}H_{25}O_6Ru$ (522.53): calcd. C 57.5, H 4.8; found C 57.3, H 4.9. Mass spectroscopy (FAB, DCM, MNBA) *m*/*z* = 523 M^+ (calcd. 522.53), 424 [M – acac]$^+$, 300 [M – Dbm]$^+$. IR (KBr): $\tilde{\nu}$ = 1520 (C=O), 1597 and 1483 (C=C), 2919 (CH sp^3) cm^{-1}. CV (DCM, 0.1 M TBAH, 0.1 V s^{-1}, vs SCE) $E_{1/2}(Ru^{III}/Ru^{II})$ = –0.767 V, $|\Delta E|$ = 0.078 V, $E_{1/2}(Ru^{III}/Ru^{IV})$ = 0.993 V, $|\Delta E|$ = 0.081 V. UV/Vis spectroscopy (DCM, 8.66×10^{-5} M): λ (ε/10^3 M^{-1} cm^{-1}) = 504 (2.2), 404 (6.5), 335 (20.6), 262 (20.6), 229 (13.5) nm. ^{1}H NMR (CD_2Cl_2): δ = 5.32 13.06 (s, 4 H, H_c), 9.94 (t, *J* = 6.9 Hz, 2 H, H_a), 6.64 (d, *J* = 6.8 Hz, 4 H, H_b), –2.46 (s, 6 H, H_p), –4.86 (s, 6 H, H_l), –26.91 (s, 2 H, H_n), –39.61 (s, 1 H, H_f) ppm. ^{13}C NMR (CD_2Cl_2): δ = 53.7, 138.46 (b), 121.79 (a), 109.22 (d), 108.32 (c), –26.28 (l), –28.52 (p) ppm.

[Ru(dbm)$_2$(acac-I)] (5) and [Ru(dbm)$_2$(acac-Br)] (6): [Ru(dbm)$_2$-(acac-I)] (**5**) was obtained by direct substitution at the 3-position of the acac ligand of [Ru(dbm)$_2$(acac)]. [Ru(dbm)$_2$(acac)] (**2**) (0.25 g, 0.4 mmol) was solubilised in toluene, and the solution was degassed with argon. *N*-Iodosuccinimide (NIS) (0.18 g, 0.78 mmol) was added and the mixture was stirred at room temp. The solution was dark orange. After 1 h, as no evolution appeared on the TLC plates (silica, toluene), the mixture was refluxed. The solution became darker (black with red gleams). NIS (0.17 g, 0.77 mmol) was added 1 h after refluxing. An hour later the last portion of NIS (0.18 g, 0.79 mmol) was added. The reaction was stopped after 4 h. To remove the excess iodine, an aqueous solution of sodium thiosulfate (0.5 M, 25 mL) was added. The mixture was then extracted with ca. 5 × 40 mL of toluene and ca. 4 × 100 mL of distilled water to wash the organic phase. All of the extracted organic portions were consolidated and the toluene was evaporated. The crude product was purified using column chromatography on silica with toluene. Dark purple crystals were obtained with a yield of 77% (0.2 g). $C_{35}H_{28}IO_6Ru$ (772.57): calcd. C 54.4, H 3.7, I 16.4; found C 53.8,

H 3.7, I 16.9. Mass spectroscopy (FAB, DCM, MNBA) *m*/*z* = 773 M^+ (calcd. 772.57), 647 [M – I]$^+$, 548 [M – acac-I]$^+$, 423 [M – Dbm–I]$^+$. IR (KBr): $\tilde{\nu}$ = 1509 (C=O), 1598, 1586 and 1482 (C=C), 2923 and 2853 (CH sp^3) cm^{-1}. CV (DCM, 0.1 M TBAH, 0.1 $V s^{-1}$, vs SCE) $E_{1/2}(Ru^{III}/Ru^{II})$ = –0.613 V, $|\Delta E|$ = 0.073 V, $E_{1/2}(Ru^{III}/Ru^{IV})$ = 1.045 V, $|\Delta E|$ = 0.074 V. UV/Vis spectroscopy (DCM, 4.92×10^{-5} M): λ ($\varepsilon/10^3$ $M^{-1} cm^{-1}$) = 562 (2.2), 414 (10.6), 331 (36.7), 257 (27.9), 228 (23.1) nm. ^{1}H NMR (CD_2Cl_2): δ = 5.32, 12.45 (s, 4 H, H_i), 11.92 (s, 4 H, H_c), 9.83 (t, *J* = 6.8 Hz, 2 H, H_k), 9.60 (t, *J* = 6.8 Hz, 2 H, H_a), 6.55 (d, *J* = 6.7 Hz, 4 H, H_b), 6.52 (d, *J* = 6.7 Hz, 4 H, H_j), –1.49 (s, 6 H, H_l), –41.08 (s, 2 H, H_f) ppm. ^{13}C NMR (CD_2Cl_2): δ = 53.7, 138.44 (j), 136.86 (b), 123.43 (a), 122.24 (k), 113.08 (d), 109.55 (c), 108.00 (i), 102.54 (h), 6.46 (l) ppm.

[Ru(dbm)$_2$(acac-Br)] (**6**) was also obtained by a direct substitution on the 3-position of the acac ligand of [Ru(dbm)$_2$(acac)]. [Ru(dbm)$_2$(acac)] (**2**) (0.36 g, 0.55 mmol) was solubilised in dichloromethane, and the solution was degassed with argon. *N*-bromosuccinimide (NBS) (0.1 g, 0.56 mmol) was solubilised in dichloromethane and was added dropwise to the solution. The mixture was stirred at room temp. The solution gradually became darker (black with red gleams). The reaction was stopped after the entire addition of NBS, and the solution was evaporated to dryness. The crude product was purified using column chromatography on silica with toluene. Black crystals were obtained with a yield of 89% (0.4 g). $C_{35}H_{28}BrO_6Ru$ (725.57): calcd. C 57.9, H 3.9, Br 11.0; found C 57.9, H 3.9, Br 11.0. Mass spectroscopy (FAB, DCM, MNBA) *m*/*z* = 727 M^+ (calcd. 725.57), 647 [M – Br]$^+$, 548 [M – acac-Br]$^+$. IR (KBr): $\tilde{\nu}$ = 1521 (C=O), 1598, 1586 and 1483 (C=C), 2923 (CH sp^3) cm^{-1}. CV (DCM, 0.1 M TBAH, 0.1 $V s^{-1}$, vs. SCE) $E_{1/2}(Ru^{III}/Ru^{II})$ = –0.608 V, $|\Delta E|$ = 0.074 V, $E_{1/2}(Ru^{III}/Ru^{IV})$ = 1.058 V, $|\Delta E|$ = 0.073 V. UV/Vis spectroscopy (DCM, 5.17×10^{-5} M): λ ($\varepsilon/10^3$ $M^{-1} cm^{-1}$) = 556 (2.4), 412 (11.6), 331 (41.0), 258 (30.6), 228 (22.8) nm. ^{1}H NMR (CD_2Cl_2): δ = 5.32, 12.38 (s, 4 H, H_i), 12.26 (s, 4 H, H_c), 9.79 (t, *J* = 6.9 Hz, 2 H, H_k), 9.67 (t, *J* = 6.9 Hz, 2 H, H_a), 6.62 (d, *J* = 6.7 Hz, 4 H, H_j), 6.50 (d, *J* = 6.7 Hz, 4 H, H_b), –1.76 (s, 6 H, H_l), –40.61 (s, 2 H, H_f) ppm. ^{13}C NMR (CD_2Cl_2): δ = 53.7, 138.32 (b), 137.03 (j), 123.57 (a), 122.42 (k), 112.33 (d), 110.15 (c), 107.82 (i), 102.73 (h), –0.05 (l) ppm.

Supporting Information (see footnote on the first page of this article): X-ray crystallographic files in CIF format for compounds **1**–**4** and **6**; ORTEP drawings of **2**, **3** and **4**; Table of crystallographic data for **1**–**4** and **6**; Table with selected bond lengths and bond angles for **1**–**4** and **6**; cyclic voltammetry of **1**, **2**, **5** and **6** (CH_2Cl_2, 0.1 M TBAH, 0.1 $V s^{-1}$). UV/Vis spectra of complexes **1**–**3** in CH_2Cl_2. UV/Vis spectra of complexes **1**, **2**, **5** and **6** in CH_2Cl_2. ^{1}H NMR spectra of complexes **1**–**3**, **5** and **6** in CD_2Cl_2. ^{13}C NMR spectra of complexes **1**–**3**, **5** and **6** in CD_2Cl_2.

Acknowledgments

The authors thank the Centre National de la Recherche Scientifique (CNRS) and the World Premier International (WPI), Materials Nanoarchitectonics (MANA) program for financial support. Y. B. and X. B. thank the Agence Nationale pour la Recherche (ANR), Conception et Simulation (COSINUS) program through the SAMSON (*s*ystem for *a*daptive *m*odeling and *s*imulation of *n*ano *o*bjects) project.

[1] D. Astruc, C. Ornelas, J. R. Aranzaes, *J. Inorg. Organomet. Polym. Mater.* **2008**, *18*, 4–17.
[2] V. Balzani, A. Credi, M. Venturi, *Chem. Eur. J.* **2008**, *14*, 26–39.
[3] J. W. Canary, S. Mortezaei, J. A. Liang, *Coord. Chem. Rev.* **2010**, *254*, 2249–2266.
[4] M. C. Dul, E. Pardo, R. Lescouezec, Y. Journaux, J. Ferrando-Soria, R. Ruiz-Garcia, J. Cano, M. Julve, F. Lloret, D. Cangussu, C. L. M. Pereira, H. O. Stumpf, J. Pasan, C. Ruiz-Perez, *Coord. Chem. Rev.* **2010**, *254*, 2281–2296.
[5] V. A. Friese, D. G. Kurth, *Curr. Opin. Colloid Interf. Sci.* **2009**, *14*, 81–93.
[6] J. K. H. Hui, M. J. MacLachlan, *Coord. Chem. Rev.* **2010**, *254*, 2363–2390.
[7] C. P. Myers, M. E. Williams, *Coord. Chem. Rev.* **2010**, *254*, 2416–2428.
[8] C. C. You, R. Dobrawa, C. R. Saha-Moller, F. Würthner, in: *Supermolecular Dye Chemistry*, **2005**, vol. 258, p. 39–82.
[9] L. Grill, *J. Phys. Condens. Matter* **2010**, *22*, 084023.
[10] M. Yu, W. Xu, Y. Benjalal, R. Barattin, E. Laegsgaard, I. Stensgaard, M. Hliwa, X. Bouju, A. Gourdon, C. Joachim, T. R. Linderoth, F. Besenbacher, *Nano Res.* **2009**, *2*, 254–259.
[11] T. Zambelli, S. Goudeau, J. Lagoute, A. Gourdon, X. Bouju, S. Gauthier, *ChemPhysChem* **2006**, *7*, 1917–1920.
[12] P. J. Low, *Dalton Trans.* **2005**, 2821–2824.
[13] C. J. Villagomez, O. Guillermet, S. Goudeau, F. Ample, H. Xu, C. Coudret, X. Bouju, T. Zambelli, S. Gauthier, *J. Chem. Phys.* **2010**, *132*, 074705.
[14] B. Calmettes, S. Nagarajan, A. Gourdon, Y. Benjalal, X. Bouju, M. Abel, L. Porte, R. Coratger, *J. Phys. Chem. C* **2009**, *113*, 21169–21176.
[15] O. Guillermet, E. Niemi, S. Nagarajan, X. Bouju, D. Martrou, A. Gourdon, S. Gauthier, *Angew. Chem. Int. Ed.* **2009**, *48*, 1970–1973.
[16] C. J. Villagomez, T. Zambelli, S. Gauthier, A. Gourdon, C. Barthes, S. Stojkovic, C. Joachim, *Chem. Phys. Lett.* **2007**, *450*, 107–111.
[17] X. Lu, K. W. Hipps, X. D. Wang, U. Mazur, *J. Am. Chem. Soc.* **1996**, *118*, 7197–7202.
[18] M. Lastapis, M. Martin, D. Riedel, L. Hellner, G. Comtet, G. Dujardin, *Science* **2005**, *308*, 1000–1003.
[19] L. Lafferentz, F. Ample, H. Yu, S. Hecht, C. Joachim, L. Grill, *Science* **2009**, *323*, 1193–1197.
[20] M. S. Alam, M. Stocker, K. Gieb, P. Muller, M. Haryono, K. Student, A. Grohmann, *Angew. Chem. Int. Ed.* **2010**, *49*, 1159–1163.
[21] S. Guo, S. A. Kandel, *J. Phys. Chem. Lett.* **2010**, *1*, 420–424.
[22] Y. H. Lu, R. Quardokus, C. S. Lent, F. Justaud, C. Lapinte, S. A. Kandel, *J. Am. Chem. Soc.* **2010**, *132*, 13519–13524.
[23] Z. Q. Wei, S. Guo, S. A. Kandel, *J. Phys. Chem. B* **2006**, *110*, 21846–21849.
[24] K. Petukhov, M. S. Alam, H. Rupp, S. Stromsdorfer, P. Muller, A. Scheurer, R. W. Saalfrank, J. Kortus, A. Postnikov, M. Ruben, L. K. Thompson, J. M. Lehn, *Coord. Chem. Rev.* **2009**, *253*, 2387–2398.
[25] P. Albores, L. D. Slep, L. S. Eberlin, Y. E. Corilo, M. N. Eberlin, G. Benitez, M. E. Vela, R. C. Salvarezza, L. M. Baraldo, *Inorg. Chem.* **2009**, *48*, 11226–11235.
[26] P. R. Andres, R. Lunkwitz, G. R. Pabst, K. Bohn, D. Wouters, S. Schmatloch, U. S. Schubert, *Eur. J. Org. Chem.* **2003**, 3769–3776.
[27] A. Carella, C. Coudret, G. Guirado, G. Rapenne, G. Vives, J. P. Launay, *Dalton Trans.* **2007**, 177–186.
[28] E. Figgemeier, L. Merz, B. A. Hermann, Y. C. Zimmermann, C. E. Housecroft, H. J. Guntherodt, E. C. Constable, *J. Phys. Chem. B* **2003**, *107*, 1157–1162.
[29] V. Ganesh, V. Lakshminarayanan, *J. Phys. Chem. B* **2005**, *109*, 16372–16381.
[30] E. Hubner, N. V. Fischer, F. W. Heinemann, U. Mitra, V. Dremov, P. Muller, N. Burzlaff, *Eur. J. Inorg. Chem.* **2010**, 4100–4109.
[31] L. Latterini, G. Pourtois, C. Moucheron, R. Lazzaroni, J. L. Bredas, A. Kirsch-De Mesmaeker, F. C. De Schryver, *Chem. Eur. J.* **2000**, *6*, 1331–1336.

[32] K. Liu, X. H. Wang, F. S. Wang, *Acs Nano* **2008**, *2*, 2315–2323.
[33] L. C. Mayor, A. Saywell, G. Magnano, C. J. Satterley, J. Schnadt, J. N. O'Shea, *J. Chem. Phys.* **2009**, *130*, 164704.
[34] K. Seo, A. V. Konchenko, J. Lee, G. S. Bang, H. Lee, *J. Am. Chem. Soc.* **2008**, *130*, 2553–2559.
[35] G. Vives, G. Rapenne, *Tetrahedron* **2008**, *64*, 11462–11468.
[36] G. Vives, J. M. Tour, *Acc. Chem. Res.* **2009**, *42*, 473–487.
[37] I. R. Baird, S. J. Rettig, B. R. James, K. A. Skov, *Can. J. Chem.* **1999**, *77*, 1821–1833.
[38] T. Hashimoto, A. Endo, N. Nagao, G. P. Sato, K. Natarajan, K. Shimizu, *Inorg. Chem.* **1998**, *37*, 5211–5220.
[39] Y. Hoshino, S. Higuchi, J. Fiedler, C. Y. Su, A. Knodler, B. Schwederski, B. Sarkar, H. Hartmann, W. Kaim, *Angew. Chem. Int. Ed.* **2003**, *42*, 674–677.
[40] M. Maruyama, N. Sonoyama, Y. Kaizu, *J. Phys. Chem.* **1994**, *98*, 5332–5337.
[41] H. Sato, T. Taniguchi, A. Nakahashi, K. Monde, A. Yamagishi, *Inorg. Chem.* **2007**, *46*, 6755–6766.
[42] J. Tamura, Y. Satsu, D. Fukuhara, K. Shimizu, G. P. Sato, *Inorg. Chim. Acta* **1995**, *236*, 37–42.
[43] S. E. Grillo, H. Tang, C. Coudret, S. Gauthier, *Chem. Phys. Lett.* **2002**, *355*, 289–293.
[44] S. Stepanow, N. Lin, J. V. Barth, *J. Phys. Condens. Matter* **2008**, *20*, 184002.
[45] F. Chiaravalloti, L. Gross, K. H. Rieder, S. M. Stojkovic, A. Gourdon, C. Joachim, F. Moresco, *Nat. Mater.* **2007**, *6*, 30–33.
[46] E. Abad, Y. J. Dappe, J. I. Martinez, F. Flores, J. Ortega, *J. Chem. Phys.* **2011**, *134*, 044701.
[47] A. Endo, M. Kajitani, M. Mukaida, K. Shimizu, G. P. Sato, *Inorg. Chim. Acta* **1988**, *150*, 25–34.
[48] A. Endo, K. Shimizu, G. P. Sato, M. Mukaida, *Chem. Lett.* **1984**, 437–440.
[49] Y. Kasahara, Y. Hoshino, K. Shimizu, G. P. Sato, *Chem. Lett.* **1990**, 381–384.
[50] I. R. Baird, B. R. Cameron, R. T. Skerlj, *Inorg. Chim. Acta* **2003**, *353*, 107–118.
[51] A. Endo, K. Shimizu, G. P. Sato, *Chem. Lett.* **1985**, 581–584.
[52] Y. Kasahara, Y. Hoshino, M. Kajitani, K. Shimizu, G. P. Sato, *Organometallics* **1992**, *11*, 1968–1971.
[53] S. Munery, J. Jaud, J. Bonvoisin, *Inorg. Chem. Commun.* **2008**, *11*, 975–977.
[54] H. H. Nguyen, N. Hoang, U. Abram, *Transit. Met. Chem.* **2010**, *35*, 89–93.
[55] P. Wang, J. E. Miller, L. M. Henling, C. L. Stern, N. L. Frank, A. L. Eckermann, T. J. Meade, *Inorg. Chem.* **2007**, *46*, 9853–9862.
[56] F. Ample, C. Joachim, *Surf. Sci.* **2006**, *600*, 3243.
[57] K. A. Jorgensen, R. Hoffmann, *J. Am. Chem. Soc.* **1986**, *108*, 1867–1876.
[58] P. Sautet, C. Joachim, *Phys. Rev. B* **1988**, *38*, 12238.
[59] M. Yu, N. Kalashnyk, R. Barattin, Y. Benjalal, M. Hliwa, X. Bouju, A. Gourdon, C. Joachim, E. Laegsgaard, F. Besenbacher, T. R. Linderoth, *Chem. Commun.* **2010**, *46*, 5545–5547.
[60] T. Choi, S. Bedwani, A. Rochefort, C. Y. Chen, A. J. Epstein, J. A. Gupta, *Nano Lett.* **2010**, *10*, 4175–4180.
[61] U. G. E. Perera, H. J. Kulik, V. Iancu, L. da Silva, S. E. Ulloa, N. Marzari, S. W. Hla, *Phys. Rev. Lett.* **2010**, *105*, 106601.
[62] G. D. Scott, D. Natelson, *Acs Nano* **2010**, *4*, 3560–3579.
[63] D. Chylarecka, C. Wackerlin, T. K. Kim, K. Muller, F. Nolting, A. Kleibert, N. Ballav, T. A. Jung, *J. Phys. Chem. Lett.* **2010**, *1*, 1408–1413.
[64] S. Loth, M. Etzkorn, C. P. Lutz, D. M. Eigler, A. J. Heinrich, *Science* **2010**, *329*, 1628–1630.
[65] R. Wiesendanger, *Rev. Mod. Phys.* **2009**, *81*, 1495–1550.
[66] A. J. M. Duisenberg, *Utrecht University*, Utrecht, The Netherlands, **1998**.
[67] M. C. Burla, R. Caliandro, M. Camalli, B. Carrozzini, G. L. Cascarano, L. de Caro, C. Giacovazzo, G. Polidori, R. Spagna, *J. Appl. Crystallogr.* **2005**, *38*, 381–388.
[68] L. J. Farrugia, *J. Appl. Crystallogr.* **1999**, *32*, 837–838.
[69] G. M. Sheldrick, *Acta Crystallogr., Sect. A* **2008**, *64*, 112–122.
[70] *Bruker*, Madison, Wisconsin, USA, **2001**.
[71] G. M. Sheldrick, *Program SADABS*, University of Göttingen, Germany, **1996**.

Received: February 3, 2011
Published Online: May 3, 2011

